Title: Potent and selective cytotoxic and anti-inflammatory gold(III) compounds containing cyclometallated phosphine sulfide ligands.

Authors: Suresh Kumar Bhargava; T. Srinivasa Reddy; Deep Pooja; Steven H. Privér; Rodney B. Luwor; Nedaossadat Mirzadeh; Shwathy Ramesan; Sistla Ramakrishna; Shailaja Karri; Madhusudana Kuncha

To be cited as: 10.1002/chem.201903388

Link to VoR: https://doi.org/10.1002/chem.201903388

Potent and selective cytotoxic and anti-inflammatory gold(III) compounds containing cyclometallated phosphine sulfide ligands.

T. Srinivasa Reddy,[‡[a]] Deep Pooja,[‡[a,b]] Steven H. Privér,[[a]] Rodney B. Luwor,*[[c]] Nedaossadat Mirzadeh,*[[b]] Shwathy Ramesan,[[d]] Sistla Ramakrishna,[[b]] Shailaja Karri,[[b]] Madhusudana Kuncha,[[b]] Suresh K. Bhargava*[[a]]

Abstract: The cycloaurated phosphine sulfide complexes [Au{κ^2-2-$C_6H_4P(S)Ph_2$}$_2$][AuX_2] [X = Cl (**2**), Br (**3**), I (**4**)] and [Au{κ^2-2-$C_6H_4P(S)Ph_2$}$_2$]PF_6 (**5**) were prepared and thoroughly characterized. The compounds are stable under physiological-like conditions, showed excellent cytotoxicity against a broad range of cancer cell lines, and remarkable cytotoxicity in 3D tumor spheroids. Mechanistic studies with cervical cancer (HeLa) cells indicate that the cytotoxic effects of the compounds involve inhibition of thioredoxin reductase and induction of apoptosis through mitochondrial disruption. *In vivo* experiments in nude mice bearing HeLa xenografts showed that treatment with compounds **4** and **5** resulted in significant inhibition of tumor growth (35.8 and 46.9%, respectively), better than that of cisplatin (29%). The newly synthesized gold complexes were also evaluated for their *in vitro* and *in vivo* anti-inflammatory activity using LPS-activated macrophages and carrageenan-induced hind paw edema models on rats, respectively.

Introduction

Since the discovery in the 1960s of the cytotoxic properties of the square planar platinum(II) complex cisplatin,[1] there has been much interest in the field of metal-based anti-cancer therapeutics. Despite the success and wide-spread clinical use of cisplatin for the treatment of cancer, particularly ovarian and testicular cancer, its limited selectivity results in undesirable side effects such as renal failure, reduced bone marrow function and blood cell production.[2] Consequently, this prompted research into other metal complexes which may prove active towards cancer cells with minimal detrimental effects to normal cells. Gold(III) being isoelectronic with, and able to form isostructural complexes to, platinum(II) soon received interest. In contrast to platinum(II), however, gold(III) complexes exhibited poor stability, light sensitivity, and were readily reduced under physiological conditions and this line of research soon faltered. Some two decades later, interest in gold(III) complexes as anti-cancer agents was renewed by reports of the cycloaurated complex [$AuCl_2$(damp)] [damp = 2-{(dimethylamino)methyl}phenyl] and its derivatives, which were stable towards reduction and active towards a range of human cancer cell lines;[3,4] their cytotoxic effects against several human cancer cell lines were comparable to, or in some cases, greater than cisplatin. Perhaps more importantly, they displayed activity towards cisplatin-resistant cell lines.

Cyclometallation has been proposed as an effective strategy to increase the stability of gold complexes under physiological conditions, restricting undesired intracellular redox reactions as a result of the strong gold-carbon σ-bond.[5] This strategy has been successfully applied to the preparation of a number of cycloaurated gold complexes containing C-N, C-N-N and C-N-C ligands (shown in Figure 1).[5,6]

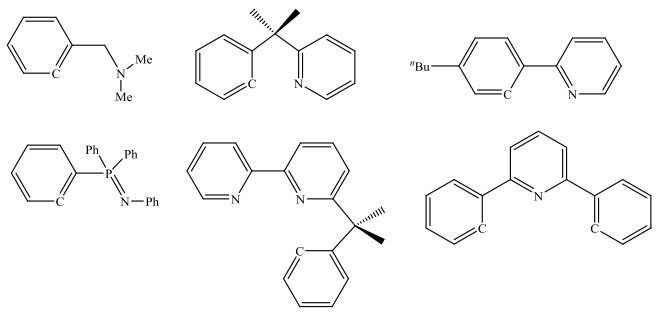

Figure 1. Bidentate C-N and tridentate C-N-N and C-N-C ligands used for the development of cycloaurated anti-cancer gold(III) complexes.

Among these ligands, the iminophosphorane has enabled the development of a unique class of gold(III) complexes (**A-C** in Figure 2) whose stability in solution can be easily monitored by ^{31}P NMR spectroscopy.[7,8] Complexes **A** and **B** exhibit high *in vitro* stability, while **C** is only stable for 24 hours. In all cases, these gold(III) compounds possess high toxicity towards Jurkat T-cell acute lymphoblastic leukemia cells and B-CLL cells.

[a] Centre for Advanced Materials & Industrial Chemistry (CAMIC), School of Science, RMIT University, GPO BOX 2476, Melbourne 3001, Australia. Email: suresh.bhargava@rmit.edu.au; nedaossadat.mirzadeh@rmit.edu.au
[b] Applied Biology Division, CSIR-Indian Institute of Chemical Technology, Hyderabad, India.
[c] Department of Surgery, Royal Melbourne Hospital, University of Melbourne, Melbourne, Victoria 3052, Australia. rluwor@unimelb.edu.au
[d] School of Engineering, RMIT University, Melbourne, Victoria 3001, Australia.
‡ equal contribution.
Electronic Supplementary Information (ESI) available:
See DOI:

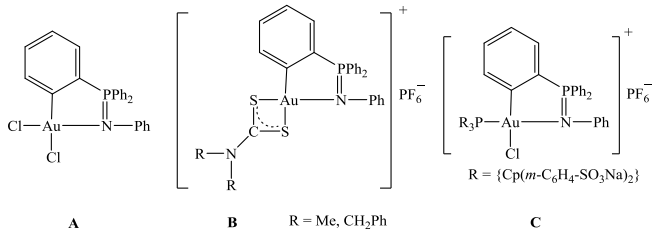

Figure 2. Examples of anti-cancer gold(III) complexes containing cycloaurated iminophosphorane ligands.

In alignment with our current research in developing gold complexes[9] for the treatment of cancer,[10-15] and inspired by the promising results of complexes containing iminophosphorane ligands, we were interested in preparing cycloaurated compounds containing closely related phosphine sulfide ligands. The preparation of the monocyclic gold(III) compounds $[AuCl_2\{\kappa^2\text{-}2\text{-}C_6H_4P(S)R_2\}]$ (R = Ph, NEt_2) has been reported, from which the thiosalicylate derivative, $[Au(1,2\text{-}SC_6H_4CO_2)\{\kappa^2\text{-}2\text{-}C_6H_4P(S)NEt_2\}]$, was synthesized.[16] Cytotoxicity studies show that the parent complex containing phenyl substituents is essentially inactive against the P388 murine leukemia cell line, but better activity was achieved in the NEt_2 and thiosalicylate derivatives. In light of these results, we have extended this class of compound to include a range of complexes containing two cycloaurated triphenylphosphine sulfide ligands (shown in Figure 3). The anti-cancer properties and mechanism of action for these gold(III) complexes representing a C-S cycloaurated moiety were investigated towards a wide range of cancer cells, the results of which are presented here.

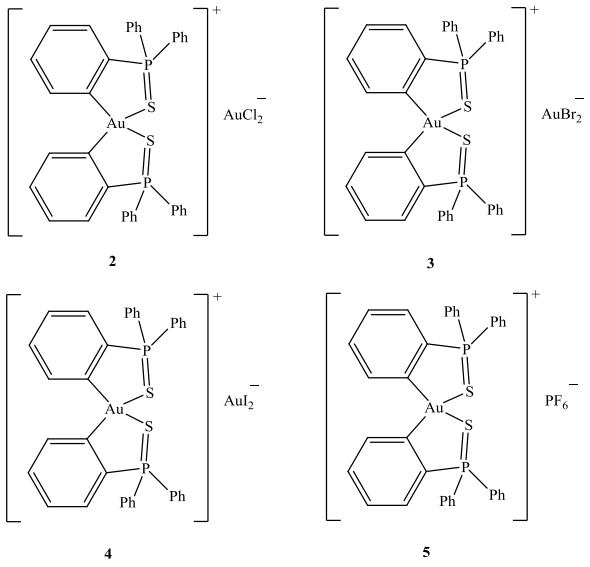

Figure 3. Gold(III) complexes containing cycloaurated triphenylphosphine sulfide ligands.

Results and Discussion

Chemistry

Reaction of $2\text{-}Me_3SnC_6H_4P(S)Ph_2$ with [AuCl(tht)] in dichloromethane gave the dinuclear digold(I) complex $[Au_2\{\mu\text{-}2\text{-}C_6H_4P(S)Ph_2\}_2]$ (**1**) as a poorly soluble solid in almost quantitative yield (Scheme 1). Compound **1** showed the expected aromatic multiplets at δ 6.8-7.8 in the ^{1}H NMR spectrum and a singlet resonance at δ 48.2 in the ^{31}P NMR spectrum (Figures S1-S2). In the structure of **1**, confirmed by X-ray crystallography (Figure 4), a pair of approximately linearly coordinated gold(I) atoms are bridged by two $C_6H_4P(S)Ph_2$ ligands in a head-to-tail arrangement forming a 10-membered ring. As a result of a slight twist of the bridging ligands, the Au···Au separation in **1** [2.8664(3) Å] is significantly smaller than that in the structurally similar complex $[Au_2(\mu\text{-}2\text{-}C_6H_4CH_2PPh_2)_2]$ [3.0035(9) Å],[17] and more closely resembles the Au···Au separation in the 8-membered ring complex $[Au_2(\mu\text{-}2\text{-}C_6H_4PPh_2)_2]$ [2.8594(3) Å].[18]

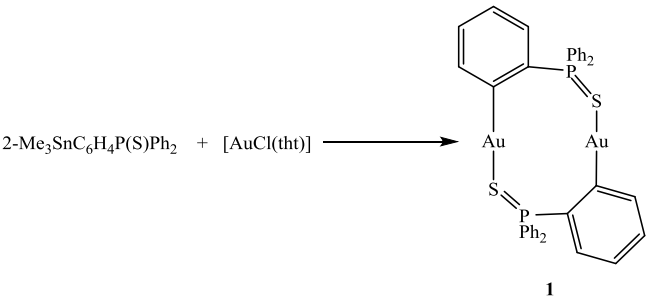

Scheme 1. Synthesis of digold(I) complex $[Au_2\{\mu\text{-}2\text{-}C_6H_4P(S)Ph_2\}_2]$ (**1**).

Oxidative addition of Cl_2 (as $PhICl_2$), Br_2 and I_2 to **1** afforded the ionic gold(I)-gold(III) complexes $[Au\{\kappa^2\text{-}2\text{-}C_6H_4P(S)Ph_2\}_2][AuX_2]$ [X = Cl (**2**), Br (**3**), I (**4**)] in 80-90% yield (Scheme 2). Complexes **2-4** each showed a singlet resonance at δ 56 in their ^{31}P NMR spectra, comparable to that observed for $[AuCl_2\{\kappa^2\text{-}2\text{-}C_6H_4P(S)Ph_2\}_2]$[16] and a peak at *m/z* 783.08 in their mass spectra, corresponding to the $[Au\{\kappa^2\text{-}2\text{-}C_6H_4P(S)Ph_2\}_2]^+$ fragment (Figures S4-S14). In the case of **2**, the ^{31}P NMR spectrum also showed two equally intense singlet resonances at δ 52.8 and 46.5, indicating the presence of *ca.* 17% of a second species. Attempts to separate or identify this species were unsuccessful, but it is believed to be the dinuclear gold(I)-gold(III) complex $[Au\{\mu\text{-}2\text{-}C_6H_4P(S)Ph_2\}_2AuCl_2]$, derived by oxidation of one of the gold atoms in **1** with retention of the bridging framework. Similar behavior has been observed for the oxidative addition of halogens to $[Au_2(\mu\text{-}2\text{-}C_6H_4CH_2PPh_2)_2]$.[17]

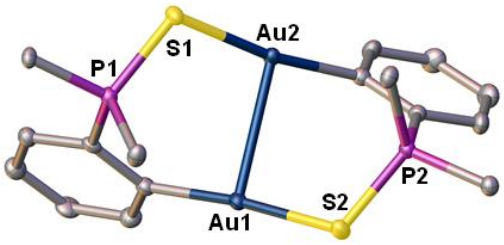

Figure 4. Molecular structure of $[Au_2\{\mu\text{-}2\text{-}C_6H_4P(S)Ph_2\}_2]$ (**1**). Ellipsoids show 50% probability levels. Hydrogen atoms and the disordered CH_2Cl_2 of crystallization have been omitted for clarity. Only the *ipso* carbon atoms of the phenyl rings are shown. Selected bond lengths (Å) and angles (°): Au(1)–Au(2) 2.8664(3), P(1)–S(1) 2.0164(16), P(2)–S(2) 2.0121(16), S(1)–Au(2) 2.3377(13), S(2)–Au(1) 2.3267(13), P(1)–S(1)–Au(2) 107.37(6), P(2)–S(2)–Au(1) 108.15(7), C(1)–Au(1)–S(2) 174.16(13), C(19)–Au(2)–S(1) 171.03(13).

The PF_6^- analog of **2-4**, $[Au\{\kappa^2\text{-}2\text{-}C_6H_4P(S)Ph_2\}_2]PF_6$ (**5**), was prepared from the reaction of $2\text{-}Me_3SnC_6H_4P(S)Ph_2$ with $[AuCl_3(tht)]$ and subsequent treatment with $TlPF_6$. Like that observed for complexes **2-4**, complex **5** showed a singlet resonance at δ 56 in its ^{31}P NMR spectrum (with an additional septet at δ 144 due to the PF_6^- ion) and a peak at *m/z* 783 in its mass spectrum (Figures S15-S18). Consistent with the spectroscopic results, the molecular structures of **4** and **5** were also confirmed by X-ray crystallography and are shown in Figures 5 and 6, respectively. As expected, the geometry about the gold(III) atom is approximately square planar and the metrical parameters for the $[Au\{\kappa^2\text{-}2\text{-}C_6H_4P(S)Ph_2\}_2]^+$ cation are almost identical in the two structures.

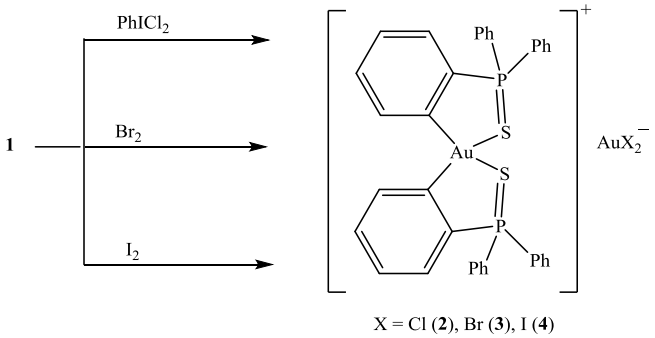

Scheme 2. Synthesis of the gold(I)-gold(III) complexes $[Au\{\kappa^2\text{-}2\text{-}C_6H_4P(S)Ph_2\}_2][AuX_2]$ (**2-4**).

Stability studies of the gold complexes under physiological-like conditions

It has been reported that gold complexes are vulnerable to ligand exchange and reduction reactions in physiological conditions.[5,19] Therefore, we investigated the stability of the newly synthesized complexes **2-5** under physiological-like conditions by monitoring the absorption spectra in tris buffered saline solutions (50 mM Tris, 150 mM NaCl, pH 7.2) and cell culture medium over 72 h.[20,21] As shown in Figure 7A and Figure S19, complexes **4** showed no significant time dependent spectral changes either in TBS or in cell culture medium, indicating the complex is stable under physiological-like conditions. In contrast, the spectra for complexes **2**, **3** and **5** (in cell culture medium) showed a slight decrease in absorbance over 72 h incubation. Complex **1** proved to be insoluble in the tris buffered saline solution, therefore its biological activity was not investigated further.

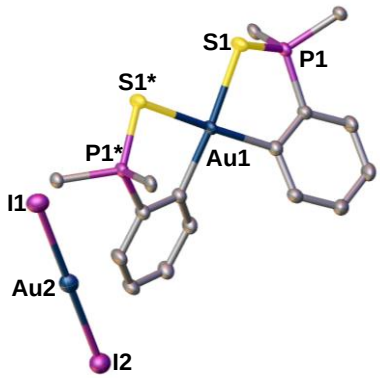

Figure 5. Molecular structure of $[Au\{\kappa^2\text{-}2\text{-}C_6H_4P(S)Ph_2\}_2][AuI_2]$ (**4**). The structure indicates *ca*. 2% of the $[AuI_2]^-$ counter ion has been replaced by I^-. Ellipsoids show 50% probability levels. Hydrogen atoms have been omitted for clarity and only the *ipso* carbon atoms of the phenyl rings are shown. Asterisks indicate atoms generated by symmetry. Selected bond lengths (Å) and angles (°): P(1)–S(1) 2.0242(9), S(1)–Au(1) 2.3998(6), Au(2)–I(1) 2.5479(5), Au(2)–I(2) 2.5421(5), S(1)–Au(1)–S(1*) 87.24(3), C(1)–Au(1)–C(1*) 92.74(13), P(1)–S(1)–Au(1) 94.01(3), I(1)–Au(2)–I(2) 180.0.

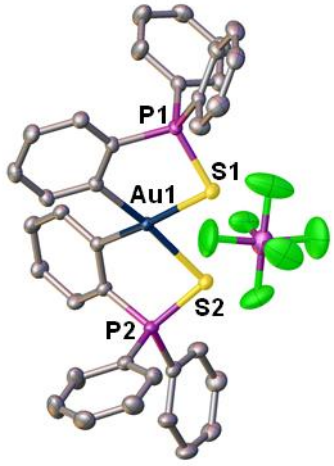

Figure 6. Molecular structure of $[Au\{\kappa^2\text{-}2\text{-}C_6H_4P(S)Ph_2\}_2]PF_6$ (**5**). Ellipsoids show 50% probability levels. Hydrogen atoms have been omitted for clarity. Only one molecule in the asymmetric unit is shown. Selected bond lengths (Å) and angles (°): P(1)–S(1) 2.0227(8), P(2)–S(2) 2.0240(8), S(1)–Au(1) 2.4048(6), S(2)–Au(1) 2.4116(6), S(1)–Au(1)–S(2) 87.67(2), C(1)–Au(1)–C(19) 94.04(8), P(2)–S(2)–Au(1) 91.53(3), P(1)–S(1)–Au(1) 92.59(3).

Glutathione plays an important role in the inactivation of the anti-cancer drug cisplatin and many other metal-based drugs.[22]

Therefore, determining the stability of metal complexes in the presence of glutathione is a crucial requirement in preclinical development. The 5,5-dithiobis-(2-nitrobenzoic acid) (DTNB) assay was carried out to determine the stability of complexes **2-5** in the presence of glutathione.

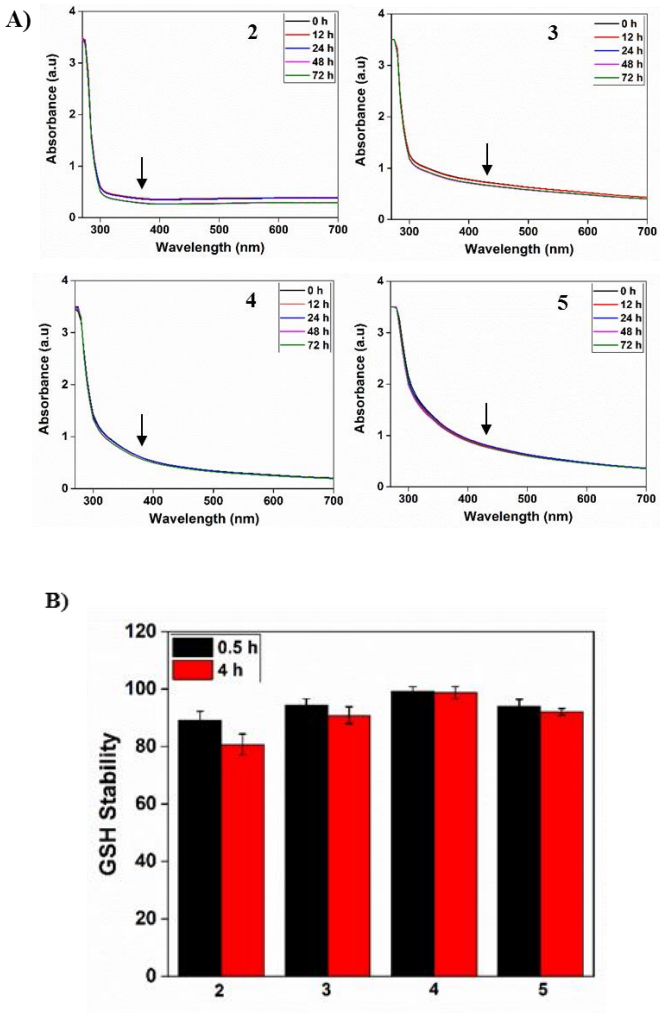

Figure 7. Stability of the gold complexes **2-5** under physiological-like conditions. A) Electronic absorption spectra of the gold complexes (20 µM) in phosphate buffered saline (pH 7.4) over 72 h. B) Stability of the gold complexes in the presence of glutathione.

In this assay, DTNB reacts with a thiol yielding one equivalent of 2-nitro-5-thiobenzoic acid (TNB) which can be measured photometrically.[23] The reaction of the gold complexes with the thiol group of cysteine in glutathione would lower the amount of free thiol available to react with DTNB. An excess of the gold complexes were incubated with glutathione at 37 ºC for 30 min and 4 h. Interestingly, complexes **3-5** did not influence the reaction significantly and can thus be considered as stable against glutathione under biologically similar conditions, which is highly desirable in the development of novel metal-based chemotherapeutics. Only compound **2** showed a moderate inhibition of approximately 11 and 21% after 0.5 and 4h, respectively (Figure 7).

Interaction with Human Serum Albumin (HSA)

Human serum albumin is the major protein in the blood responsible for acidity and pressure, as well as the metabolism of drugs. The interaction of metal complexes with HSA influences the overall drug distribution and excretion profile of the metal complexes and can be studied using a fluorescence method. The intrinsic fluorescence of HSA mainly results from the tryptophan residue (Trp-214) in the hydrophobic cavity and the fluorescence of Trp-214 changes when HSA interacts with other molecules. Therefore, the interactions of the gold complexes with HSA was investigated using fluorescence spectroscopy.[24] The intensity of the characteristic broad emission band at 342 nm decreased markedly with increasing concentration of the complexes, indicating an interaction between the gold complexes and HSA (Figure 8). The variation in the intensity of the emission maximum could result from the changes in the protein conformations or a quenching effect by the complexes. However, the maximum emission wavelength of HSA did not change during the interaction with complexes **2**, **3** and **5**, suggesting that the complexes interacted with hydrophobic region located inside HSA without altering the polarity around the tryptophan residues. In contrast, a red shift of the emission maximum in the fluorescence spectrum of the albumin was observed after incubation with complex **4**, suggesting an increased hydrophobicity around the tryptophan residues.[25]

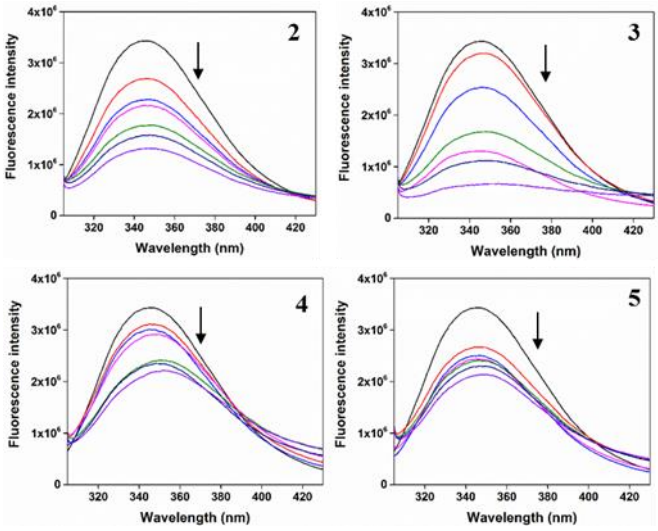

Figure 8. Interaction of the gold complexes **2-5** with human serum albumin (HSA). Fluorescence emission spectra of HSA in the absence and presence of increasing concentrations of gold complexes (0, 10, 20, 40, 60, 80 and 100 µM, respectively) in Tris HCl/NaCl buffer (pH = 7.2).

***In vitro* anti-cancer activity**

The cytotoxic potential of the synthesized gold complexes **2-5** was assessed using the MTT (3-(4,5-dimethylthiazol-2-yl)-2,5-diphenyltetrazolium bromide) assay against a wide range of

human cancer cell lines and one noncancerous cell line and compared to cisplatin. The results of these cytotoxicity assays are expressed as IC_{50} values and are listed in Table 1. Structurally, complexes **2-5** contain the same cationic gold fragment and differ only in the anion, thereby enabling us to study the counter ion effect on the anti-tumor activities of the complexes. Also, complexes **2-4** contain the gold(I) counter anions $AuCl_2^-$, $AuBr_2^-$ and AuI_2^-, respectively, whereas complex **5** has a PF_6^- counter ion allowing for a comparison of the cytotoxicity of dinuclear complexes with a mononuclear complex. As shown in Table 1, the newly synthesized gold complexes displayed excellent *in vitro* anti-cancer activities and showed more potent and broader spectrum of cytotoxicity on the tested cancer cell lines as compared to cisplatin, which had a narrow spectrum of activity (only active on HeLa, HT-1080 and PC-3 cells). The complexes exhibited excellent cancer cell growth inhibition with IC_{50} values in the range of 0.44-3.38 µM. In particular, complex **4** containing the AuI_2^- counter ion demonstrated superior *in vitro* cytotoxicity toward all the tested cancer cells with IC_{50} values in the range 0.44-1.27 µM with approximately 24-fold higher cytotoxicity than cisplatin towards D24 melanoma cancer cells and 10- and 7-fold higher cytotoxicity against colon (HCT-116) and cervical (HeLa) cancer cells, respectively. Complex **4** also showed 6- and 5-fold more selective cytotoxicity towards cervical and prostate cancer cells, respectively, compared to the non-cancerous Hek-293 cells. Complex **5** with the PF_6^- counter ion also possessed an excellent cytotoxicity profile, similar to those for complexes **2-4** with gold(I) counter ions. Further, among the complexes with gold(I) counter ions, complex **4** containing AuI_2^- showed the best activity. Taken together, these results indicate that cationic gold(III) and anionic gold(I) ions are essential for the high anti-cancer activity.

Table 1. *In vitro* cytotoxicity (IC_{50} values, µM) of the gold complexes **2-5** and cisplatin after 72 h incubation towards various cell lines.

	MDAMB-231	HeLa	HT-1080	HCT-116	D24	PC-3	Hek-293
2	2.64± 0.15	2.71± 0.32	1.36± 0.09	3.38± 0.89	2.48± 0.46	1.56 ±0.68	3.23 ±0.25
3	1.24± 0.07	2.31± 0.13	0.93± 0.05	3.19± 0.18	2.44± 0.26	0.59 ±0.12	3.55 ±0.16
4	1.08± 0.13	0.44± 0.07	0.79± 0.23	1.27± 0.23	0.97± 0.08	0.54 ±0.19	2.87 ±0.87
5	1.81± 0.07	1.86± 0.25	0.65± 0.06	2.05± 0.21	2.22± 0.11	1.05 ±0.22	4.26 ±0.35
Cis-pt	17.56± 0.87	3.04± 0.23	0.54± 0.16	13.5± 1.68	23.5± 1.68	4.60 ±1.23	4.81 ±0.25

MDAMB-231, Breast; HeLa, Cervical; HT-1080, Fibrosarcoma; HCT-116, Colon; D-24, Melanoma; PC-3, Prostate; Hek-293, Human embryonic kidney cells (non-cancerous).

Anti-cancer activity in 3D multicellular spheroids

3D Multicellular tumor spheroids (MCTS) are used to simulate the *in vivo* tumor microenvironment which provides higher complexity than the standard 2D monolayer cultures due to their physiological relevance to solid tumors.[26,27] Therefore, to validate the anti-tumor activity of the synthesized gold complexes in an *in vivo* tumor environment, cervical cancer cells (HeLa) were grown in ultra-low attachment (ULA) plates for 2 days to generate 3D multicellular spheroids which were treated with IC_{50} concentrations of the gold complexes.

Figure 9 shows the morphological changes in the MCTS after 72 h of treatment with the gold complexes. Live and dead cells were differentiated by calcein (green) and propidium iodide (red) fluorescence, respectively. In live cells, ubiquitous intracellular esterase enzymes convert the non-fluorescent cell-permeant calcein AM to the intensely green fluorescent calcein. In the case of dead cells, propidium iodide enters the cells through damaged membranes, binds to nucleic acids and produces 40-fold enhanced red fluorescence. Treatment with the gold complexes led to disruption and disaggregation of the MCTS structures; disaggregation was particularly extensive after treatment with complexes **2**, **3** and **5**.

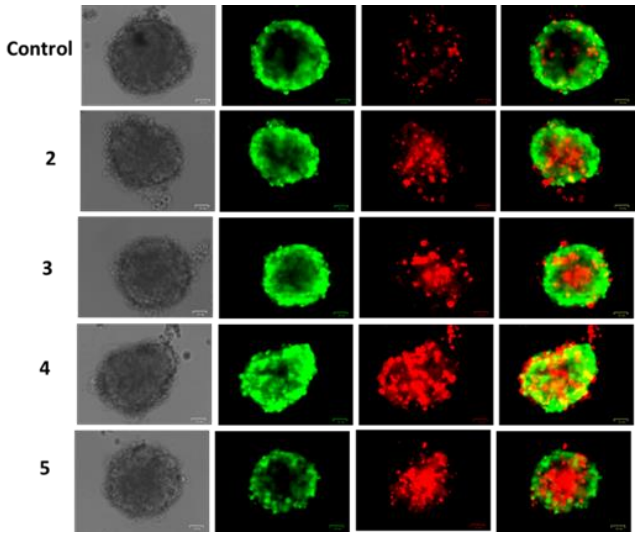

Figure 9. Anti-tumor activity of complexes **2-5** towards 3D multicellular tumor spheroids of HeLa cancer cells. Cellular spheroids formed in 96 well ultra-low attachment plates were treated with IC_{50} concentrations of the gold complexes for 3 days and stained with calcein AM (live)/propidium iodide (dead). Green (live cells); red (dead cells).

Further, live/dead staining indicated that untreated spheroids emitted a steady green fluorescence from the live cells and low levels of red fluorescence (dead cells). After treatment with complexes **2**-**5**, bright-red fluorescence was observed indicating severe cell death had occurred. Among these, treatment with compound **4** resulted in the greatest cell death. These results revealed that the synthesized gold complexes are effective in killing cancer cells in physiologically relevant 3D multicellular spheroids.

Migration and invasion studies

Endothelial cell migration is a key step in the progression of tumors and the metastasis process.[28] Therefore, the discovery of drugs that can simultaneously inhibit cancer growth and decreases the endothelial cell motility is essential for efficient cancer therapy. A wound-healing assay was carried out to evaluate the anti-migratory effect of the gold complexes, while the invasive capability of the cells in the presence of the gold complexes was determined by transwell assays.[29,30] The wound-healing process of endothelial HUVEC cells was triggered by scratching a cell monolayer, followed by treatment with IC_{50} concentrations of the gold complexes. The closure of wounds was observed immediately and after 24 and 48 h treatment through phase contrast microscopy. As shown in Figure 10A, the untreated control HUVEC cells migrate in a time dependent manner and the wound area was almost closed after 48 h incubation. In contrast, treatment with the gold complexes resulted in a significant inhibition of wound closure and thus the migration of HUVEC cells in comparison to the control cells at both time points. Among the gold compounds, the highest percentage of migration inhibition was observed for complex **2**. The invasion assay was carried out using HUVEC cells as these cells are highly invasive and aggressive compared to HeLa cells. As shown in Figure 10B, treatment with complexes **2**-**5** led to strong inhibition of HUVEC cell invasion through the matrigel coated membrane and a reduced number of invaded cells were observed. In summary, these results demonstrate the potential of the anti-migratory and anti-invasive effect of complexes **2**-**5**.

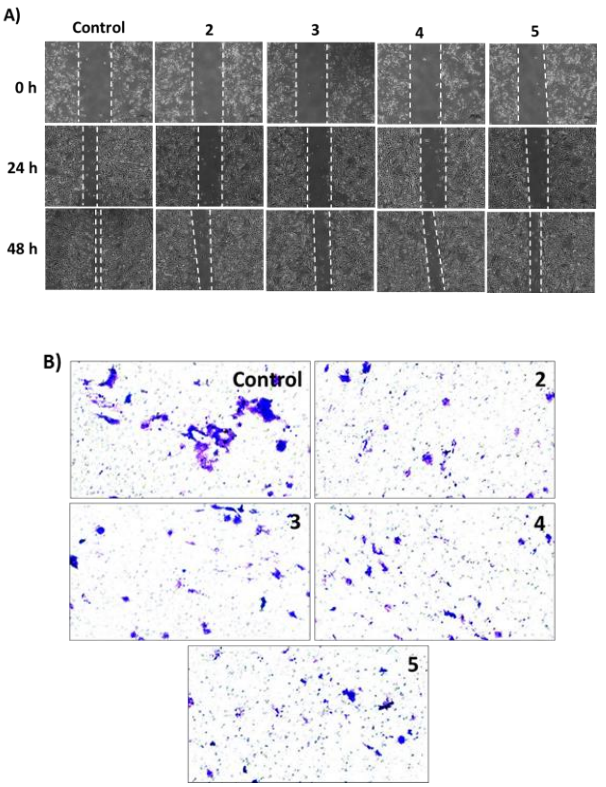

Figure 10. Anti-migratory and anti-invasive effect of gold complexes **2-5**. (A) Wound healing assay: Microscopic images of the wound gaps of HUVEC cells after 0, 24 and 48 h after treatment with the gold complexes. (B) Transwell migration assay. HUVEC cells which are invaded through the matrigel-coated chamber were stained with 0.25% crystal violet and the photographs were taken using an inverted microscope.

Disruption of actin assembly polymerization studies

Cell migration is the basis of tumor cell invasion and metastasis. Malignant cancer cells invade adjacent tissues and vasculature using their intrinsic migratory ability leading to metastasis by the formation of membrane protrusions. The polymerization of sub-membrane actin filaments is a vital step for the formation of cell membrane protrusions.[31] Given that the gold complexes inhibited cell migration, we assessed the effect of these complexes on actin polymerization. In this assay, HeLa cells were treated with the gold complexes for 24 h and stained with rhodamine phalloidin, a F-actin protein specific green fluorescent probe. As shown in Figure 11, the control cells displayed elongated fibres with expanded lamellipodia whereas the cells treated with the gold complexes were granulated and condensed without the broad lamellipodia, indicating the complexes inhibit the migration through disruption of actin assembly.

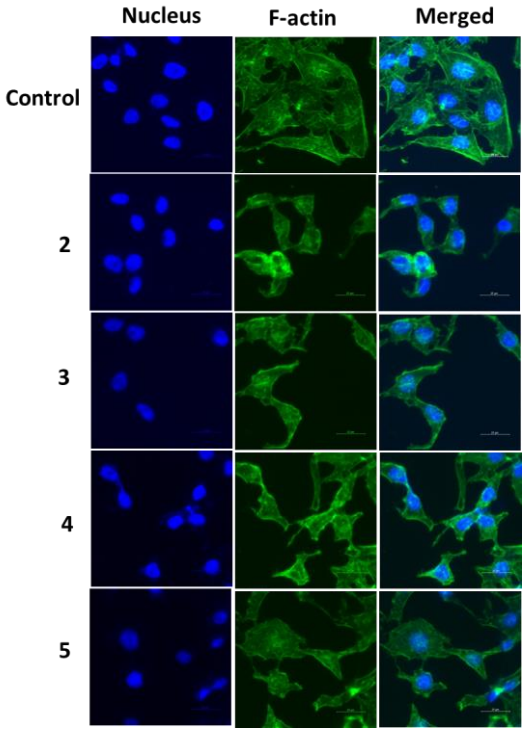

Figure 11. Effect of complexes **2-5** on actin (stress fibre) polymerization of HeLa cells assessed by staining with an actin specific dye. The control cells exhibited intact stress fibres whereas treatment with the gold complexes led to condensed actin filaments.

Cellular uptake studies

The amount of gold taken up by the cells is responsible for the cytotoxicity and was determined using ICP-MS.[32] As shown in Figure 12, more gold is accumulated in the HeLa cells after treatment with the binuclear gold complex **4** containing the AuI_2^- counter ion compared to cells treated with complexes **2** ($AuCl_2^-$) and **3** ($AuBr_2^-$) and **5** (PF_6^-). After 8 hours incubation, intracellular gold concentration in HeLa cells was approximately 3 times higher than those treated with complex **2**. The cellular uptake experiments demonstrate that the varying uptake levels observed for the gold complexes may be due to differences in stability under physiological conditions and hydrophobicity. Complex **4** with a higher stability exhibits an increased intracellular uptake and higher toxicity towards cancer cells. The observed differences may also be related to the stability of the complexes in the presence of glutathione. For example, compounds **4** is stable and is not reduced in the presence of glutathione whereas complexes **2** undergo reduction. These results indicate that the counter ions are also important to the properties of the complexes and potential intracellular processing that might take place under physiological conditions.

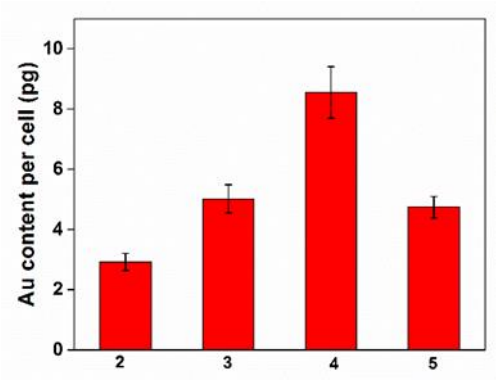

Figure 12. Gold uptake by cervical cancer cells (HeLa) after exposure to complexes **2-5** for 8 h analyzed by ICP-MS.

Thioredoxin reductase inhibition

Thioredoxin reductase (TrxR) is a selenoenzyme that plays an important role in regulating cellular events such DNA synthesis, cell proliferation, apoptosis and cellular anti-oxidantion.[33] The thioredoxin system reacts with reactive oxygen species (ROS) and helps in overcoming cellular oxidative stress. Overexpression of TrxR is linked with the development of many tumors with increased cell anti-oxidant potential, drug resistance and poor cancer cell prognosis.[34] Therefore, targeting the TrxR system has emerged as a promising strategy for anti-cancer therapy. To evaluate the TrxR inhibition activity of the metal complexes and to determine the possible relationship between TrxR inhibition and cell growth inhibition, the TRxR inhibition assay was carried out on HeLa cells treated with complexes **2-5**.[35] After treatment with 1 µM concentrations of complexes **2-5**, a significant reduction of thioredoxin reductase activity in HeLa cells was noted, with an observed inhibition of 61.3, 65.2, 73.5 and 71.6%, respectively, after 12 hrs incubation (Figure 13). Complex **4**, which showed potent cell growth inhibitory effects compared to the other metal complexes, also showed better TrxR inhibitory activities *in vitro*. The observed TrxR inhibitory effect in HeLa cell lysates indicate that these complexes are suitable candidates for the selective targeting of this enzyme.

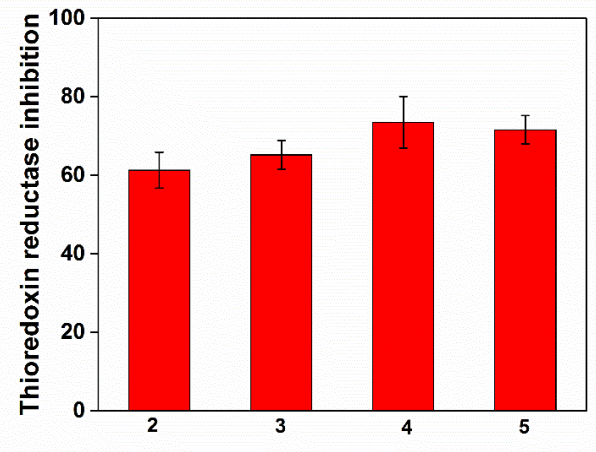

Figure 13. Effect of the gold complexes on thioredoxin reductase inhibition. Thioredoxin reductase activity from HeLa whole cell lysates was monitored following incubation with 1 µM of complexes **2-5** for 12 hrs.

Apoptosis inducing effects

Translocation of phosphatidylserine from the inner layer of the plasma membrane to the outer layer of the membrane occurs during the process of apoptosis.[36] This externalization of phosphatidylserine can be detected by AnnexinV-FITC staining.[37] Propidium iodide is used to stain the dead cells and to differentiate drug induced apoptosis or necrosis. HeLa cells treated with complexes **2-5** displayed an increase in Annexin-V positive cells. After incubation for 48 h, apoptotic cells accounted for 36-41% of the total cells, indicating that apoptosis was a pathway of the cytotoxicity of the metal complexes (Figure 14A). The apoptosis effect of the gold complexes was also evident from the morphological changes *viz* nuclear shrinkage, chromatin condensation and apoptotic body formation in HeLa cells (Figure 14B).[38] Moreover, the effects of the gold complexes on the mitochondrial membrane potential (ΔΨm) were investigated using JC-1, since mitochondrial membrane disruption and loss of ΔΨm have been reported to play a key role in apoptosis.[39] As shown in Figure 14C, a significant increase in green fluorescence due to JC-1 monomers was observed after incubation with the gold complexes, indicating the collapse of ΔΨm in HeLa cells.

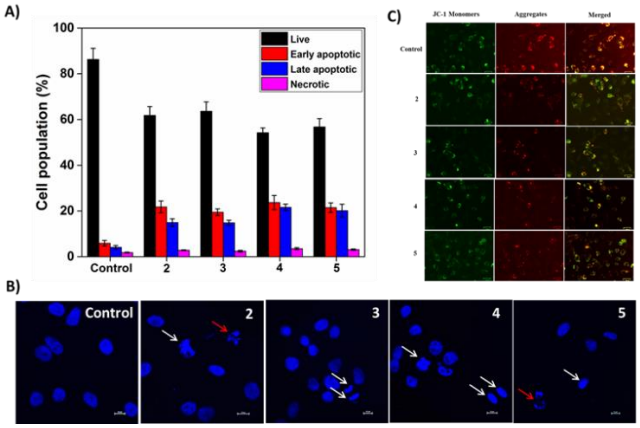

Figure 14. Induction of apoptosis in HeLa cells. (A) Annexin V-FITC propidium iodide double staining assay. HeLa cells treated with IC_{50} concentrations of the gold complexes for 48 h were stained with Annexin V-FITC and propidium iodide. (B) Analysis of morphological changes in HeLa cells exposed to IC_{50} concentrations of the gold complexes. The apoptotic cells are shown as bright blue. (C) The collapse of mitochondrial membrane potential. HeLa cells incubated with IC_{50} concentrations of the metal complexes were stained with JC-1 dye and the images were captured with a fluorescence microscope.

In vivo anti-tumor activity

The anti-tumor experiments using mice xenografts were approved by the Animal Ethics Committee at the University of Melbourne (Animal Ethics Application 1814422). The *in vivo* anti-tumor activity was examined in nude mice bearing HeLa xenografts with 1 mg/kg of compounds **4**, **5** and cisplatin through an intraperitoneal injection once every 3 days. The results, shown in Figures 15A and 15B, indicate that significant tumor volume inhibition (35.8 and 46.9%) was observed after treatment with complexes **4** and **5**, respectively, compared to those treated with solvent control. In addition, no mouse death or body weight loss was observed after treatment with the gold complexes at this dose. In contrast, treatment with cisplatin resulted in 29% tumor volume inhibition. We also analyzed the expression of Ki-67, a cell proliferation marker in tumor sections by immunohistochemistry.[40] As shown in Figures 15C and 15D, compared with the control group, treatment with the metal complexes resulted in less Ki-67 staining, suggesting that the gold complexes inhibit tumor proliferation.

Anti-inflammatory activity

Cytokine expression

Auranofin, a gold(I) phosphine compound, has been prescribed for the treatment of rheumatoid arthritis as a disease-modifying anti-rheumatic drug (DMARD). It has been reported that auranofin is able to slow down the progression of the disease by suppressing inflammation through inhibition of endotoxin induced IL-1β and TNF-α production in the monocytes and macrophages.[41,42] Therefore, to evaluate the *in vitro* anti-inflammatory potential of the newly synthesized gold complexes, their ability to diminish the release of the pro-inflammatory cytokines TNF-α and IL-1β in PMA/LPS stimulated macrophages derived from the U937 cell line was determined.[43] The maximum non-toxic concentration of each individual gold compound was used to access the release of TNF-α and IL-1β using ELISA kits. The results were compared with prednisolone, a steroidal anti-inflammatory drug which supresses the expression of pro- inflammatory cytokines.

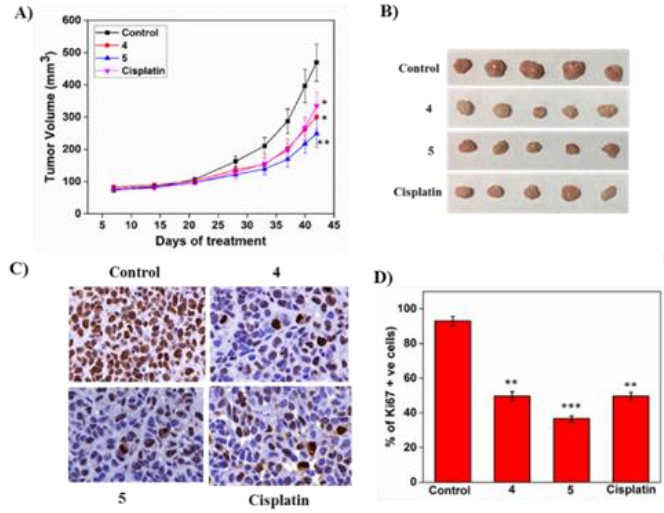

Figure 15. Anti-tumor activity of complexes **4**, **5** and cisplatin in mice bearing HeLa xenografts. A) Changes of tumor volume (mm^3) after intraperitoneal administration of metal complexes (1 mg/kg). Data represents the mean ± standard error of five mice per group. The control group received an equal volume of PBS with vehicle control (DMSO). B) Representative images of tumors after 42 days of treatment. C & D) Expression of Ki-67 in tumor tissue was analyzed by immunofluorescence staining.

Table 2. Percentage inhibition of TNF-α and IL-1β by complexes **2-5** and standards at their non-toxic concentration.

	% Inhibition of cytokines		IC_{50} (μM)	
Compound	**TNF-α**	**IL-1β**	**TNF-α**	**IL-1β**
2	59	99	3.266± 0.032	1.691± 0.082
3	88.6	79.5	2.141± 0.194	1.684± 0.231
4	93.8	86.2	0.8173± 0.0543	0.4857± 0.048
5	90	70	0.5745± 0.0255	0.06316± 0.024
Auranofin	95.3	87	0.908 ± 0.25	0.908 ± 0.13
Prednisolone	97	95	0.0358± 0.002	0.1545± 0.001

The results of the study (Table 2) showed that complexes **2-5** inhibited the secretion of TNF-α and IL-1β after LPS treatment. Complexes **3**-**5** exhibited a greater inhibitory effect towards TNF-

α expression than IL-1β, whereas complex **2** was more effective in IL-1β attenuation. All the complexes inhibited the expression of both cytokines to a similar extent to that of the prednisolone and auranofin standards. IC_{50} values (concentration at which the compound exhibits 50% inhibition of TNF-α and IL-1β) were determined from a dose-response curve (concentration vs. response curve). The results clearly show that the expression of inflammatory-related cytokines TNF-α and IL-1β was greatly influenced by the gold complexes.

***In vivo* anti-inflammatory activity**

Inspired by the significant *in vitro* anti-inflammatory activities of the gold complexes, the *in vivo* anti-inflammatory activity was evaluated using the acute carrageenan-induced paw edema models in rats. The formation of edema is one of the symptoms of acute inflammation.[42] Auranofin was used as a reference standard. Indomethacin, a typical cyclooxygenase inhibitor that shows negligible effect on the cytokine expression, was used as a secondary positive standard. All the compounds were administered as an oral suspension prepared using gum acacia at a dose of 10 mg/kg body weight 3 h prior to carrageenan administration. The changes in paw volume (i.e. swelling or edema) were measured using a plethysmometer after 3 h of carrageenan injection. The differences in paw volume before and after treatment and percent inhibition are shown in Table 3.

Table 3. Differences and % inhibition in paw volume of Wistar rat after treatment at a dose of 10 mg/kg body weight.

Formulations	Difference in paw volume after treatment (mL)	% inhibition in paw volume
Control	1.48 ± 0.05	-
2	1.2 ± 0.03	4.51 ± 1.28
3	1.32 ± 0.04	10.81 ± 2.56
4	1.14 ± 0.03	22.84 ± 2.96
5	1.46 ± 0.07	3.65 ± 2.36
Indomethacin	0.636 ± 0.06	57.03 ± 4.53
Auranofin	0.984 ± 0.03	21.28 ± 2.25

Indomethacin and auranofin showed 57.03 and 21.28 % inhibition in paw edema, respectively, whereas complexes **2-5** resulted in 4.85, 10.81, 22.84, and 3.65% inhibition, respectively. Complex **2**, **3** and **5** only showed a weak anti-inflammatory activity in the animal models whereas the activity of complex **4** was moderate and comparable to that of auranofin.

Conclusions

In summary, we have shown that the newly synthesized cycloaurated phosphine sulfide complexes exhibit interesting biological properties. All the compounds (**2-5**) exhibit remarkable anti-proliferative activities against a broad range of cancer cell lines with IC_{50} values in the range of 0.44-3.38 μM, with complex **4** being the most active. Stability studies indicate complex **4** containing the AuI_2^- is more stable compared to **2** and **3**, which is consistent with the hard/soft acid/base theory, and may account for its higher cytotoxicity. The cytotoxicity results also show that the cationic fragment $[Au\{\kappa^2\text{-}2\text{-}C_6H_4P(S)Ph_2\}_2]^+$, present in all the tested compounds, shows moderate activity which can be increased by replacing the PF_6^- counter ion by AuI_2^-. Notably, complex **4** showed superior *in vitro* cytotoxicity towards all the tested cancer cells with approximately 24-fold higher cytotoxicity than cisplatin towards D24 melanoma cancer cells and 10- and 7-fold higher cytotoxicity against colon (HCT-116) and cervical (HeLa) cancer cells, respectively. Complex **4** also showed 6- and 5-fold greater selectivity towards cervical and prostate cancer cells compared to the non-cancerous Hek-293 cells. The compounds exhibit their cytotoxicity through strong inhibition of TrxR and mitochondrial damage. More importantly, two of the synthesized gold complexes (**4** and **5**) have demonstrated their *in vivo* efficacy in inhibiting tumor growth in mice bearing HeLa xenografts. Additionally, complexes **2-4** inhibit the secretion of pro-inflammatory cytokines in LPS activated microphases. Further, complex **4** was also equally effective in *in vivo* studies to the clinically used anti-arthritis drug auranofin. In light of the results reported here, we believe that cycloaurated phosphine sulfide complexes represent a promising and interesting class of potent and selective cytotoxic agents with anti-inflammatory properties.

Experimental

General comments

[AuCl(tht)],[44] $[AuCl_3(tht)]$,[45] $PhICl_2$[46] and $2\text{-}Me_3SnC_6H_4P(S)Ph_2$[47] were prepared following literature methods. ^1H (300 MHz) and ^{31}P (121 MHz) NMR spectra were obtained as $CDCl_3$ solutions on a Bruker Avance 300 spectrometer at room temperature. Chemical shifts are referenced to residual solvent signals (^1H) or external 85% H_3PO_4 (^{31}P) and coupling constants (*J*) are given in Hz. ESI and high resolution ESI mass spectra were acquired on an Applied Biosystem 3200 MDS Sciex Q-trap and Perkin-Elmer AxION 2 TOF spectrometer, respectively. CHN analyses were carried out in the Chemical Engineering Department at RMIT University using a Perkin-Elmer 2400 Series II CHNS/O analyser.

Synthesis

Preparation of $[Au_2\{\mu\text{-}2\text{-}C_6H_4P(S)Ph_2\}_2]$ (1)

To a solution of $2\text{-}Me_3SnC_6H_4P(S)Ph_2$ (1.48 g, 3.24 mmol) in CH_2Cl_2 (10 mL) was added [AuCl(tht)] (1.04 g, 3.24 mmol) in CH_2Cl_2 (10 mL). The mixture was stirred for 10 min, during which time a solid formed. Hexane (20 mL) was added to the suspension and the pale yellow solid was filtered off. The solid was washed with hexane and dried *in vacuo* (1.56 g, 98%). ^1H NMR: δ 6.84-7.01 (m, 4H), 7.20-7.29 (m, 2H), 7.52-7.81 (m, 22H). ^{31}P NMR: δ 48.2 (s). ESI-MS (*m/z*): 981.0 $[M]^+$, 783.0 $[M\text{-}Au]^+$.

Preparation of $[Au\{\kappa^2\text{-}2\text{-}C_6H_4P(S)Ph_2\}_2][AuCl_2]$ (2)

To a suspension of $[Au_2\{\mu\text{-}2\text{-}C_6H_4P(S)Ph_2\}_2]$ (767 mg, 0.78 mmol) in CH_2Cl_2 (50 mL) cooled to -78°C was added $PhICl_2$ (215 mg, 0.78 mmol) in CH_2Cl_2 (10 mL). The color of the mixture turned orange and the solution was left to stir at -78°C for 30 mins, then allowed to warm to room temperature and stirred for a further 30 mins, during which time the color faded to pale yellow. The solution was filtered through Celite and toluene was added to the filtrate. The volume of the solution was reduced *in vacuo* until a white precipitate began to form and the mixture was allowed to stand for 10 min. The white solid was filtered off, washed with toluene then recrystallized from CH_2Cl_2/hexane (662 mg, 81%). ^1H NMR: δ 6.78-7.22 (m, 2H), 7.29-7.59 (m, 6H), 7.60-7.94 (m, 20H). ^{31}P NMR: δ 56.8 (major product, s), 52.8 (minor product, s), 46.5 (minor product, s).

Anal. Calcd. for $C_{36}H_{28}Au_2Cl_2P_2S_2$: C 41.12, H 2.68; Found: C 41.39, H 2.45. Positive HR ESI-MS (*m/z*): 783.0777. Calcd. For $C_{36}H_{28}AuP_2S_2$: 783.0773.

Preparation of [Au{κ²-2-$C_6H_4P(S)Ph_2$}$_2$][$AuBr_2$] (3)

To a suspension of [Au_2{μ-2-$C_6H_4P(S)Ph_2$}$_2$] (500 mg, 0.51 mmol) in CH_2Cl_2 (60 mL) cooled to -78°C was added a solution of Br_2 (28 μL, 0.54 mmol) in CH_2Cl_2 (10 mL) dropwise. The color of the mixture turned orange and the solution was left to stir at -78°C for 30 mins, then allowed to warm to room temperature and stirred for a further 30 mins, during which time the color of the solution faded to yellow. After filtration through Celite, toluene (20 mL) was added to the filtrate and the volume of the solution was reduced *in vacuo*, precipitating out a white solid. This solid was filtered off, washed with toluene and recrystallized from CH_2Cl_2/hexane (528 mg, 91%). ^{1}H NMR: δ 7.08-7.21 (m, 2H), 7.36-7.59 (m, 6H), 7.62-7.86 (m, 20H). ^{31}P NMR: δ 56.8 (s). Anal. Calcd. for $C_{36}H_{28}Au_2Br_2P_2S_2$: C 37.91, H 2.47; Found: C 38.20, H 2.28. Positive HR ESI-MS (*m/z*): 783.0768. Calcd. For $C_{36}H_{28}AuP_2S_2$: 783.0773. Negative HR ESI-MS (*m/z*): 356.8019. Calcd. for $AuBr_2$: 356.8012.

Preparation of [Au{κ²-2-$C_6H_4P(S)Ph_2$}$_2$][AuI_2] (4)

To a suspension of [Au_2{μ-2-$C_6H_4P(S)Ph_2$}$_2$] (500 mg, 0.51 mmol) in CH_2Cl_2 (60 mL) cooled to -78°C was added a solution of I_2 (130 mg, 0.51 mmol) in CH_2Cl_2 (30 mL) dropwise. The color of the mixture turned orange, then brown, and was left to stir at -78°C for 30 min, then allowed to warm to room temperature and stirred for a further 30 mins. The brown solution was filtered through Celite and toluene (20 mL) added to the filtrate. The volume of the solution was reduced *in vacuo* to give an yellow solid, which was filtered off, washed with toluene and recrystallized from CH_2Cl_2/hexane (565 mg, 90%). ^{1}H NMR: δ 7.09-7.19 (m, 2H), 7.37-7.59 (m, 6H), 7.64-7.84 (m, 20H). ^{31}P NMR: δ 56.9 (s). Anal. Calcd. for $C_{36}H_{28}Au_2I_2P_2S_2$: C 35.03, H 2.29; Found: C 35.46, H 2.03. Positive HR ESI-MS (*m/z*): 783.0754. Calcd. for $C_{36}H_{28}AuP_2S_2$: 783.0773. Negative HR ESI-MS (*m/z*): 450.7745. Calcd. for AuI_2: 450.7755.

Preparation of [Au{κ²-2-$C_6H_4P(S)Ph_2$}$_2$]PF_6 (5)

To a solution of [$AuCl_3$(tht)] (250 mg, 0.64 mmol) in CH_2Cl_2 (35 mL) cooled to -78°C was added solid 2-$Me_3SnC_6H_4P(S)Ph_2$ (600 mg, 1.31 mmol). The yellow solution was stirred at -78°C for 30 min, then allowed to warm to room temperature and stirred for a further 60 min. The bright yellow solution was filtered through Celite and the volume reduced to 5 mL. Dropwise addition of Et_2O precipitated [Au{κ²-2-$C_6H_4P(S)Ph_2$}$_2$]Cl as a pale yellow solid, which was isolated by filtration, washed with Et_2O and dried *in vacuo* (520 mg, 99%). The isolated product is sparingly soluble in organic solvents and on some occasions, was contaminated with a small amount (< 1%) of the gold(I) dimer [Au_2{μ-2-$C_6H_4P(S)Ph_2$}$_2$] (**1**) but could be used as-is for the synthesis of the PF_6 salt.

To a suspension of [Au{κ²-2-$C_6H_4P(S)Ph_2$}$_2$]Cl (498 mg, 0.61 mmol) in CH_2Cl_2 (50 mL) was added $TlPF_6$ (225 mg, 0.64 mmol) and the mixture stirred for 1.5 h, protected from light. The suspension was filtered through Celite and the solvent removed. The residue was dissolved in MeCN containing a little CH_2Cl_2 and, if necessary, filtered to remove traces of [Au_2{μ-2-$C_6H_4P(S)Ph_2$}$_2$]. The volume of the filtrate was reduced to 5 mL and dropwise addition of Et_2O precipitated a white solid. After stirring for 10 min, the solid was filtered off, washed with Et_2O and dried *in vacuo* (485 mg, 86%). ^{1}H NMR: δ 7.06-7.16 (m, 2H), 7.34-7.56 (m, 6H), 7.62-7.84 (m, 20H). ^{31}P NMR: δ 56.9 (s, 2P), -144.4 (sept, J_{PF} = 711 Hz, 1P). Anal. Calcd. for $C_{36}H_{28}AuF_6P_3S_2$: C 46.56, H 3.04; Found: C 46.81, H 2.90 Positive HR ESI-MS (*m/z*): 783.0760. Calcd. for $C_{36}H_{28}AuP_2S_2$: 783.0773. Negative HR ESI-MS (*m/z*): 144.9637. Calcd. For PF_6: 144.9642.

X-ray crystallography

Crystals of complexes **1**, **4** and **5** suitable for single-crystal X-ray diffraction were obtained from dichloromethane/hexane. A crystal was mounted on a nylon loop using a drop of inert oil (Nujol) before being transferred into a stream of cold nitrogen. The reflections were collected on a D8 Bruker diffractometer equipped with an APEX-II area detector using graphite-monochromated Mo Kα radiation (λ = 0.71073 Å) from a 1 μS micro source. For data collection and data processing, the programs SMART[48] and SAINT[49] were used, respectively, and absorption corrections using SADABS.[50] The structures were solved using direct methods and refined with full-matrix least-squares methods on F^2 using the SHELX-TL package.[51, 52] The CCDC numbers for complexes **1**, **4** and **5** are 1873195-1873197.

Absorption measurements

Absorption titration experiments for investigating the stability of the metal complexes under physiological-like conditions were performed using a UV-Visible spectrophotometer (The Agilent Cary 60). 10 mM stock solutions of the gold complexes were prepared in DMSO and diluted to 20 μM in Tris HCl/NaCl buffer (pH 7.2) or cell culture medium (DMEM with 10% FBS). Titrations were done manually using a micropipette and the change in absorbance data of the solutions were recorded over a period of 72 h.

Human serum albumin binding interactions

For fluorescence titration experiments, a solution of human serum albumin (1 mL, 10 μM in Tris HCl/NaCl buffer) was placed in a quartz cuvette and titrated with varying amounts of a stock solution of the gold complexes such that the final concentrations ranged from 0 to 100 μM. After each addition, the solution was mixed thoroughly for 30 s before measurement (λ_{ex} = 295 nm, λ_{em} = 310–580 nm).

Cell culture

The human breast carcinoma (MDAMB-231), human prostate carcinoma (PC-3), human cervical carcinoma (HeLa), human colon carcinoma (HCT-116), human fibrosarcoma (HT-1080), human melanoma (D-24), human embryonic kidney (Hek-293) and human monocytic U937 cells were obtained from American Type Culture Collection (ATCC), Manassas, USA. Dulbecco's Modified Eagle Medium (DMEM), Roswell Park Memorial Institute 1640 (RPMI) medium, foetal bovine serum (FBS), penicillin and streptomycin were purchased from Gibco, Life Technologies. Lipopolysaccharide (LPS) from Escherichia coli, phorbol myristate acetate (PMA), XTT Sodium salt and lipopolysaccharide (LPS) were purchased from Sigma-Aldrich Co, St Louis, MO, USA. Human specific TNF-α and IL-1β ELISA kits were purchased from BD Bioscience, San Diego, CA, USA.

Anti-cancer activity of gold complexes

The *in vitro* cytotoxicity of the gold complexes was determined using the MTT assay against different cancer cell lines mentioned above. The percent cell growth inhibition was determined after 72 h drug exposure and compared with cisplatin. Cells were cultured either in DMEM or RPMI medium supplemented with 10% FBS, 2 mM glutamine, penicillin (100 U/mL), and streptomycin (0.1 mg/mL) followed by incubation in a humidified 5% CO_2 incubator at 37°C. Cells were seeded in 96-well culture plates and allowed to adhere for 24 h at 37°C then incubated with varying concentrations (0.01-100 μM) of complexes **2-5** and cisplatin. After 72 h exposure, the media was replaced with serum-free media (containing 0.5 mg/mL MTT) and incubated for 4 h. The media was removed and 150 μL of DMSO was added to each individual well to dissolve the formazan crystals. The absorbance of the solutions was measured at 570 nm using a micro-plate reader. The percent cell viability was calculated using the formula % cell viability = As/Ac × 100%, where, As = absorbance of sample and Ac = absorbance of control or untreated

cells incubated under identical conditions. The half-maximal inhibitory concentration (IC_{50}) values were determined using the probit analysis software package in MS Excel.

Spheroid inhibition assay

About 5 × 10^3 HeLa cells/well were seeded in 96-well ULA (ultra-low attachment) round-bottom plates and allowed to grow for 2 days for spheroid formation. The spheroids were incubated with IC_{50} concentrations of the gold complexes for 72 h. The culture medium was replaced with fresh medium after two days while maintaining the same drug concentrations. For visualization of the live/dead cells, after 72 h of treatment the spheroids were incubated with calcein AM (2 μM) and propidium iodide (4 μM) for 30 mins and imaged under an inverted fluorescence microscope.

Wound healing assay

HeLa cells (2 × 10^5 cells/well) were seeded in a 6-well plate and allowed to adhere overnight. Wounds were created across the well using a 200 μL sterile pipette tip and then the cells were washed with PBS (phosphate buffered saline) to remove the cell debris. The cells were incubated with or without the gold complexes (at IC_{50} concentrations) in complete growth medium for 48 h. The number of cells migrated into the wound area were observed at 0 h, 24 h and 48 h of treatment using an inverted fluorescence microscope.

Transwell migration assay

The invasion ability of HUVEC cells was assessed using transwell chambers with polycarbonate filters. HeLa cells starved with serum for 24 h were collected and resuspended in medium containg 0.1% FBS. The cells were seeded in the transwells with 8 μm pores (20000 cells/well in 0.2 mL) and was inserted in the 24 well plate. To the lower chamber of the plate was added 10% FBS as chemoattractant. Cells were treated with the gold complexes for 24 h. After incubation, the cells remaining on the upper side of the transwell chamber were swabbed with a cotton tip and the cells that migrated to the lower chamber were fixed with methanol and stained with crystal violet. The images were captured using an inverted fluorescence microscope (Nikon).

Effect on F-actin

HeLa cells (2 × 10^5 cells/well) were seeded on cover slips in a 6-well plate and allowed to adhere overnight. The cells were incubated with complexes **2-5** for 24 h and then washed with PBS and fixed with 4% paraformaldehyde. The cells were treated with 0.01% Triton-X 100 and alexafluor 488 phalloidin for 1 h at room temperature, then washed with PBS to remove excess dye and further incubated with Hoechst 33242 (2 μg/mL) for 10 min at room temperature to stain the nucleus. The coverslips were then mounted with ProLong Gold anti-fade reagent (Molecular probes) and observed using a confocal microscope (Nikon).

Thioredoxin reductase inhibition

HeLa cells treated with 1 μM solution of complexes **2-5** for 5 h were collected and lysed in assay buffer. The lysates were subjected to centrifugation at 10000 x g for 15 min at 4°C after adding 1 mM protease inhibitor cocktail. The protein concentrations were determined by the Bradford method. The soluble fraction of the lysates were incubated for 30 min in assay buffer (Abcam thioredoxin reductase assay kit ab83463) before adding DTNB. The absorbance of the solutions were measured using a SpectraMax microplate reader at 412 nm. All the lysates were tested in triplicate.

Cellular uptake

HeLa cells (2 x 10^6 per flask) were seeded in 25 cm^2 cell culture flasks and allowed to grow overnight. The cells were treated with 1 μM concentrations of complexes **2-5** for 8 h and then washed with PBS. Cells were collected using Trypsin-EDTA and were lysed. The lysates were separated into two parts. One part was used for protein estimation using the Bradford method. To the second portion, concentrated HCl was added to dissolve the gold and the final solution was made to 3% HCl using ultrapure Milli Q water. The samples were analyzed for gold content using ICP-MS (Agilent).

Hoechst staining

The ability of complexes **2-5** to induce the morphological changes in the nucleus of HeLa cells was analysed by Hoechst 33242 staining. The cells (2 × 10^5) were grown on cover slips and treated with IC_{50} concentrations of the gold complexes. After 48 h, the cells were washed with PBS, fixed with 4% paraformaldehyde and stained with Hoechst 33242 (2 μg/mL) for 15 min at room temperature. The cells were washed with PBS to remove excess dye and observed under a confocal microscope (Nikon).

Annexin V-FITC/PI (propidium iodide) staining

The apoptotic potential of complexes **2-5** towards HeLa cells was investigated by annexin V and PI staining using flow cytometry (BD Accuri C6). The cells at a density of 1 × 10^5 cells/well were seeded into a 6-well plate and allowed to adhere overnight, then incubated with IC_{50} concentrations of the gold complexes. After 48 h, the cells were harvested using 0.25% Trypsin-EDTA, washed with cold PBS and suspended in 100 μL annexin V binding buffer (2.5 mM $CaCl_2$, 140 mM NaCl, 10 mM HEPES/NaOH, pH 7.4) and then incubated with 5 μL annexin V and 1 μL PI (100 μg/mL) for 15 min at room temperature. Then 10,000 cells were taken from each sample for analysis by flow cytometry.

Measurement of mitochondrial membrane potential (ΔΨm)

HeLa cells (5 × 10^5 cells/mL) were grown in 6-well plates and treated with complexes **2-5** for 48 h. The cells were washed with PBS and incubated with JC-1 (5 μg/mL) at room temperature for 30 min. After washing two times with PBS to remove excess dye, the cells were imaged using a fluorescence microscope at 20× magnification (Biorad).

***In vivo* anti-tumor activity in mice xenograft models**

Five week old female BALB/c nude mice were used for the experiments. 5 × 10^6 HeLa tumor cells were resuspended in 100 μL of RPMI medium and subcutaneously injected into both ventral flanks, anterior to the hind leg using a 29 gauge insulin syringe. The mice were monitored twice daily for 48 h for any unexpected adverse effects. The tumors were allowed to establish to approximately 50 mm^3 (as determined using electronic callipers) and the mice were then randomly separated into three groups of 5. The mice were injected with intraperitoneal doses of either the vehicle control, 1 mg/kg of complex **2**, **4** or cisplatin every three days for 42 days. Tumor volumes were measured 8 times during the 42 days period. All mice were culled after 42 days and the tumors were collected and weighed. All animal experiments were performed at the Biological Research Facility, Melbourne University in accordance with the animal ethics number 1814422. Immunohistochemical staining of mouse tumor sections were performed by the staff at the Anatomical Pathology Laboratory Services located at The Royal Children's Hospital, Melbourne, Australia, according to standard protocols.[51] The results were reported as the mean ± standard deviation (SD). Student's t-test in MS Excel was used to analyze the statistical significance.

Anti-inflammatory activity

The human monocytic cell line U937 is a widely characterized model of the mammalian cellular response to various inflammatory stimuli. U937 cells show a marked increase in the release of pro-inflammatory cytokines when differentiated by phorbol myristate acetate (PMA) and activated by lipopolysaccharide (LPS). The release of pro-inflammatory

cytokines, such as TNF-α, the β form of pro-IL-1 (IL-1β), IL-6 and IL-8, by activated leukocytes represent a crucial step in the inflammatory response that occurs in the pathogenesis of chronic diseases like rheumatoid arthritis. Therefore, U937 cells were used to evaluate the effect the gold complexes on the induction of an anti-inflammatory response. Preliminary cytotoxicity tests were performed using the XTT assay to ensure that the inhibition of cytokines is not due to the cytotoxic effect of the gold complexes. The U937 cells were exposed to different concentrations of complexes **2**-**5**, ranging from 0.156 to 10 µM for 24 h. All the compounds showed more than 80% cell viability below 1.25 µM concentration. The maximum non-toxic concentration of each individual complex was selected to study their effect on the release of pro-inflammatory cytokines.

Cell viability assay

The maximum non-toxic concentrations of the gold complexes (the concentration at which cell viability was more than 80%) was determined using the XTT tetrazolium reduction assay. U937 cells (1 x 10^4) were seeded in 96-well plate and allowed to adhere overnight. The cells were then incubated with varying concentrations of the gold complexes ranging from 0.156 µM to 10 µM for 24 h. After incubation with XTT for 4 h, the media was removed and DMSO was added to dissolve the formazan crystals. The cell viability was determined by measuring absorbance of the solution at 470 nm. The maximum non-toxic concentration was used to determine the release of pro-inflammatory cytokines.

Drug treatment and induction of inflammatory response

To differentiate cells from macrophages, 5 x 10^5 cells were seeded in a 24-well plate and incubated with PMA (60 ng/mL) overnight. The cells were then treated with complexes **2**-**5**, auranofin and prednisolone at non-toxic concentrations for 1 h. After incubation with LPS (1 µg/mL) for 24 h the supernatant was collected for determination of TNF-α and IL-1β. The concentration of TNF-α and IL-1β was quantified using an ELISA kit (BD Biosciences San Diego, CA, USA) according to the manufacturers' instructions. Prednisolone and auranofin were taken as standards. IC_{50} values (the concentration at which compound exhibits 50% inhibition of TNF-α and IL-1β) were determined using a dose-response curve (DRC, concentration vs. response curve). To plot the DRC, cells were treated with different concentrations (lower than the maximum non-toxic concentration) of complexes **2**-**5** and the release of TNF-α and IL-1β were measured.

***In vivo* anti-inflammatory activity (carrageenan-induced hind paw edema)**

The anti-inflammatory effects of the gold complexes were evaluated using the acute carrageenan-induced paw edema models in rats. All the studies on animals were performed in accordance with the guidelines of the Committee for the Purpose of Control and Supervision of Experiments on Animals (CPCSEA) under the approval and scrutiny of the Institutional Animal Ethics Committee (IAEC) of the CSIR-Indian Institute of Chemical Technology (IICT), Hyderabad, India. Male Wistar rats were acclimatized to the laboratory conditions for 7 days before initiation of the study in BIOSAFE, an animal quarantine facility of the Institute. All the animals were given free access to a standard pellet diet and fresh drinking water *ad libitum*. Animals were housed under standard laboratory conditions (12 h light, 12 h dark cycle) in polypropylene cages at 20 ± 2 ºC. Male Wistar rats (weighing 180–200 g) were randomly divided into 7 groups consisting of 6 rats in each group. Animals were pre-treated with complexes **2**-**5** (10 mg/kg), indomethacin (10 mg/kg, standard drug), auranofin (10 mg/kg, positive reference) and the control group of animals orally received saline 3 h prior to the carrageenan injection. After 3 h, 0.1 mL of 1% w/v carrageenan in isotonic saline was injected in the subplantar region of the left hind paw for both test and control group animals. Paw volumes were measured for all the rats 3 h after the administration of carrageenan using a plethysmometer. The degree of swelling induced was evaluated by the percentage change of volume of the right hind paw before and after carrageenan treatment. The anti-inflammatory activity of the formulation was calculated as percent inhibition of paw volume calculated with reference to the mean paw volume of rats in the control group.

Acknowledgements

The authors acknowledge the Micro Nano Research Facility (MNRF), RMIT University, for providing the facilities to carry out cell culture experiments.

Keywords: Gold anti-cancer • Gold anti-inflammatory • Gold(III) • Cyclometallated • Phosphine sulfide ligands

[1] B. Rosenberg, L. VanCamp, J. E. Trosko, V. H. Mansour, *Nature* **1969**, *222*, 385-386.
[2] R. Oun, Y. E. Moussa, N. J. Wheate, *Dalton Trans*. **2018**, *47*, 6645-6653.
[3] R. G. Buckley, A. M. Elsome, S. P. Fricker, G. R. Henderson, B. R. C. Theobald, R. V. Parish, B. P. Howe, L. R. Kelland, *J. Med. Chem*. **1996**, *39*, 5208-5214.
[4] R. V. Parish, B. P. Howe, J. P. Wright, J. Mack, R. G. Pritchard, R. G. Buckley, A. M. Elsome, S. P. Fricker, *Inorg. Chem*. **1996**, *35*, 1659-1666.
[5] T. Zou, C. T. Lum, C. N. Lok, J. J. Zhang, C. M. Che, *Chem. Soc. Rev*. **2015**, *44*, 8786-8801.
[6] P. Zhang, P. J. Sadler, *J. Organomet. Chem*. **2017**, *839*, 5-14.
[7] L. Vela, M. Contel, L. Palomera, G. Azaceta, I. Marzo *J. Inorg. Biochem*. **2011**, *105*, 1306-1313.
[8] N. Shaik, A. Martínez, I. Augustin, H. Giovinazzo, A. Varela-Ramírez, M. Sanaú, R. J. Aguilera, M. Contel, *Inorg. Chem*. **2009**, *48*, 1577-1587.
[9] N. Mirzadeh, M. A. Bennett, S. K. Bhargava, *Coord. Chem. Rev*. **2013**, *257*, 2250-2273.
[10] V. G. Reddy, T. S. Reddy, S. H. Privér, Y. Bai, S. Mishra, D. Wlodkowic, N. Mirzadeh, S. Bhargava, *Inorg. Chem.* **2019**, *58*, 5988-5999.
[11] T. S. Reddy, S. H. Privér, N. Mirzadeh, S. K. Bhargava, *Eur. J. Med. Chem*. **2018**, *145*, 291-301.
[12] T. S. Reddy, S. H. Privér, N. Mirzadeh, S. K. Bhargava, *J. Inorg. Biochem*. **2017**, *175*, 1-8.
[13] T. S. Reddy, S. H. Privér, V. V. Rao, N. Mirzadeh, S. K. Bhargava, *Dalton Trans*. **2018**, *47*, 15312-15323.
[14] N. Mirzadeh, S. H. Privér, A. Abraham, R. Shukla, V. Bansal, S. K. Bhargava, *Eur. J. Inorg. Chem*. **2015**, 4275-4279.
[15] N. Mirzadeh, T.S. Reddy, S. K. Bhargava, *Coord. Chem. Rev*. **2019**, *388*, 343-359.
[16] K. J. Kilpin, W. Henderson, B. K. Nicholson, *Dalton Trans*. **2010**, *39*, 1855-1864.
[17] M. A. Bennett, S. K. Bhargava, D. C. R. Hockless, F. Mohr, K. Watts, L. L. Welling, A. C. Willis, *Z. Naturforsch.* **2004**, *59B*, 1563-1569.
[18] M. A. Bennett, S. K. Bhargava, K. D. Griffiths, G. B. Robertson, W. A. Wickramasinghe and A. C. Willis, *Angew. Chem., Int. Ed. Engl.* **1987**, *26*, 258-260.

[19] L. Messori, F. Abbate, G. Marcon, P. Orioli, M. Fontani, E. Mini, T. Mazzei, S. Carotti, T. O'Connell, P. Zanello, *J. Med. Chem*. **2000**, *43*, 3541-3548.

[20] M. J. Chow, M. V. Babak, K. W. Tan, M. C. Cheong, G. Pastorin, C. Gaiddon, W. H. Ang, *Mol. Pharm.* **2018,** *15*, 3020-3031.

[21] M. J. Chow, M. V. Babak, D. Y. Q. Wong, G. Pastorin, C. Gaiddon, W. H. Ang, *Mol. Pharm.* **2016**, *13*, 2543-2554.

[22] H. H. Chen, M. T. Kuo, *Met. Based Drugs*, 2010, 2010, Article ID: 430939.

[23] R. Rubbiani, I. Kitanovic, H. Alborzinia, S. Can, A. Kitanovic, L. A. Onambele, M. Stefanopoulou, Y. Geldmacher, W. S. Sheldrick, G. Wolber, A. Prokop, S. Wolfl, I. Ott, *J. Med. Chem.* **2010**, *53*, 8608–8618.

[24] S. Tabassum, W. M. Al-Asbahy, M. Afzal, F. Arjmand, *J. Photochem. Photobiol. B.* **2012**, *114*, 132-139.

[25] N. Na, D. Q. Zhao, H. Li, N. Jiang, J. Y. Wen, H. Y. Liu, *Molecules* **2016**, *21*, 54.

[26] S. Sant and P. A. Johnston, *Drug Discov. Today: Technol*. **2017**, *23*, 27-36.

[27] G. Lazzari, P. Couvreur, S. Mura, *Polym. Chem*. **2017**, *8*, 4947-4969.

[28] F. van Zijl, G. Krupitza, W. Mikulits, *Mutat. Res. Rev. Mutat. Res.* **2011**, *728*, 23-34.

[29] C. R Justus, N. Leffler, M. Ruiz-Echevarria, L. V. Yang, *J. Vis. Exp.* **2014**, *88*, e51046.

[30] N. Kramer, A. Walzl, C. Unger, M. Rosner, G. Krupitza, M. Hengstschläger,H. Dolznig, *Mutat. Res. Rev. Mutat. Res.* **2013**, *752*, 10-24.

[31] D. D. Tang, B. D. Gerlach, *Respir. Res*. **2017**, *18*, 54.

[32] H. Scheffler, Y. You, I. Ott, *Polyhedron* **2010**, *29*, 66-69.

[33] J. E. Biaglow, R. A. Miller, *Cancer Biol. Ther.* **2005**, *4*, 6-13.

[34] G. Powis, D. Mustacich, A. Coon, *Free Rad. Biol. Med*. **2000**, *29*, 312-322.

[35] J. Fernández-Gallardo, B. T. Elie, T. Sadhukha, S. Prabha, M. Sanaú, S. A. Rotenberg, J. W. Ramos, M. Contel, *Chem. Sci*. **2015**, *6*, 5269-5283.

[36] K. Segawa, S. Nagata, *Trends Cell Biol*. **2015**, *25*, 639-650.

[37] G. Koopman, C. P. Reutelingsperger, G. A. Kuijten, R. M. Keehnen, S. T. Pals, M. H. Van Oers, *Blood* **1994**, *84*,1415-1420.

[38] A. Saraste, K. Pulkki, *Cardiovascular Res*. **2000**, *45*, 528-537.

[39] P. Chen, J. Y. Zhang, B. B. Sha, Y. E. Ma, T. Hu, Y. C. Ma, H. Sun, J. X. Shi, Z. M. Dong, P. Li, *Oncotarget*, **2017**, *8*, 27471-27480.

[40] S. Hougee, A. Sanders, J. Faber, Y. M. Graus, W. B. van den Berg, J. Garssen, H. F. Smit, M. A. Hoijer, *Biochem. Pharmacol.* **2005**, *69*, 241-248.

[41] J. Vančo, J. Gáliková, J. Hošek, Z. Dvořák, L. Paráková, Z. Trávníček, *PloS One* **2014**, 9, e109901.

[42] Z. Trávníček, P. Štarha, J. Vančo, T. Šilha, J. Hošek, P. Suchý Jr, G. Pražanová, *J. Med. Chem*. **2012**, *55*, 4568-4579.

[43] R. Junek, R. Morrow, J. I. Schoenherr, R. Schubert, R. Kallmeyer, S. Phull, R. Klöcking, *Phytomedicine* **2009**, *16*, 470-476.

[44] R. Uson, A. Laguna, M. Laguna, *Inorg. Synth*. **1989**, *26*, 85-91.

[45] A. Adé, E. Cerrada, M. Contel, M. Laguna, P. Merino, T. Tejero, *J. Organomet. Chem*., **2004**, *689*, 1788-1795.

[46] H. J. Lucas, E. R. Kennedy, *Org. Synth. Coll. Vol*. III, **1955**, 482.

[47] S. H. Privér, M. A. Bennett, A. C. Willis, S. Pottabathula, M. L. Kantam, S. K. Bhargava, *Dalton Trans*. **2014**, *43*, 12000-12012.

[48] SMART software ver. 5.625 for the CCD Detector System, Bruker AXS Inc., Madison, WI, 2001.

[49] SAINTPLUS software ver. 6.22 for the CCD Detector System, Bruker AXS Inc., Madison, WI, 2001.

[50] R. H. Blessing, *Acta Crystallogr. A*., **1995**, *51*, 33-38.

[51] G. M. Sheldrick, SHELXTL, ver. 2013/4, Universität Göttingen, Germany, 2013.

[52] G. M. Sheldrick, *Acta Crystallogr. A*. **2008**, *64*, 112-122.

Entry for the Table of Contents

RESEARCH ARTICLE

Cycloaurated phosphine sulfide complexes with anti-cancer and anti-inflammatory properties.

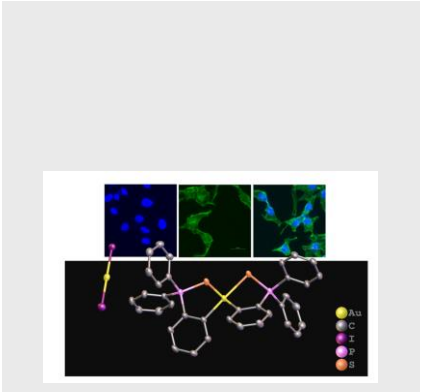

T. Srinivasa Reddy, Deep Pooja, Steven H. Privér,Rodney B. Luwor, Nedaossadat Mirzadeh,* Shwathy Ramesan, Sistla Ramakrishna, Shailaja Karri, Madhusudana Kuncha, Suresh K. Bhargava***

Page No. – Page No.

Potent and selective cytotoxic and anti-inflammatory gold(III) compounds containing cyclometallated phosphine sulfide ligands.